minerals

MDPI

Article

Mineralogical and Chemical Characteristics of Slags from the Pyrometallurgical Extraction of Zinc and Lead

Katarzyna Nowinska

Department of Applied Geology, Faculty of Mining, Safety Engineering and Industrial Automation, Silesian University of Technology, ul. Akademicka 2, 44-100 Gliwice, Poland; katarzyna.nowinska@polsl.pl

Received: 28 March 2020; Accepted: 18 April 2020; Published: 20 April 2020

Abstract: The slags derived from the fire refining of lead bullion, differ distinctly in the mineral composition, which results from the fact that these slags are end products of a series of chemical reactions (of both reduction and oxidation). The most common phases included in the refining slags are sulphates and hydrated sulphates (anglesite, gypsum, ktenasite and namuvite), oxides and hydroxides (wustite and goethite), nitrates (gerhardtite) and silicates (kirschsteinite and willemite). The other phases are sulphides and hydrated sulphides (sphalerite and tochilinite), metals (metallic Pb) and glass. Among the mineral components of these slags can be distinguished—primary mineral constituents, phase constituents formed in the ISP process and lead refining, secondary mineral constituents, formed in the landfill. The slags contain, in chemical terms, mainly FeO, CuO and SO_3, PbO, in smaller contents SiO_2, Al_2O_3 and CaO, TiO_2, MnO, MgO, K_2O, P_2O_5. The mineralogical and chemical composition indicate that slags may be a potential source of metals recovery and pyrometallurgical processing of these wastes seems to be highly rational.

Keywords: slags; mineral composition; chemical composition; pyrometallurgy; zinc; lead

1. Introduction

Pyrometallurgical extraction of zinc and lead using the Imperial Smelting Process (ISP) is based on the reduction of roasted Zn-Pb concentrate with coke at 1000 °C in a shaft furnace. The feedstock for the process is a mixture of zinc-lead concentrates; materials recycled from the process, that is, sludges, dusts, dross; secondary raw materials such as scrap zinc alloys, zinc dross, crude lead from other sources and waste, including—dusts from steel making, zinc dust and dross, zinc sludge, lead oxide, cable scrap. The diversity of feedstock implicates varying chemical and mineral composition of products and waste generated in the ISP process.

The products of the process include crude zinc and crude lead, which are then rectified (Zn) or refined (Pb). In the process of multi-stage lead fire refining, slag is produced, which is the only waste of the ISP process deposited in a landfill [1–3].

These slags contain a number of chemical constituents, of which the dominant ones are—ZnO, PbO, Fe_2O_3, CaO, SiO_2 and their content in the slag exceeds 10% [4].

The mineral composition of slags from the refining process is varied and the most common phase constituents are oxides and hydroxides (zincite ZnO, wustite FeO, hematite Fe_2O_3, goethite FeO(OH)), sulphides (sphalerite ZnS, galena PbS, pyrite FeS_2, pyrrhotite $Fe_{1-x}S$) and sulphates (anglesite PbSO4, gypsum $CaSO_4{\cdot}2H_2O$), silicates and aluminosilicates (willemite Zn_2SiO_4, olivine $(Mg,Fe)_2\ SiO_4$, (fayalite Fe_2SiO_4, kirschsteinite $CaFeSiO_4$, forsterite Mg_2SiO_4), pyroxene $AB[Si_2O_6]$ (A—Ca, Na; B—Fe, Mg, Al), melilite $Ca,Na)_2(Al,Mg,Fe^{2+})[(Al,Si)SiO_7]$) which usually form complex conglomerates or multiphase intergrowths resulting from a number of chemical processes occurring during lead refining.

These slags were also found to contain carbonates (cerussite $PbCO_3$, smithsonite $ZnCO_3$, hydrozincite $Zn_5(CO_3)_2(OH)_6$), metal alloys (Pb, Zn, Cu, Fe) and secondary minerals (e.g., gypsum $CaSO_4{\cdot}2H_2O$, rapidcreekite $Ca_2(SO_4)(CO_3){\cdot}4H_2O$, apatite $Ca_5(PO_4)_3(F,Cl,OH)$, ktenasite $ZnCu_4(SO_4)_2(OH)_6{\cdot}6H_2O$ and posnjakite $Cu_4[(OH)_6|SO_4]{\cdot}H_2O$), which crystallize after the slag is deposited in a landfill [4–11].

Due to the high concentrations of elements, including toxic metals, the refining slags deposited in a landfill may pose a potential threat to the natural environment on the one hand and a source for their extraction on the other [11–16].

The basis for determining the potential negative environmental impact of the slags and for indicating the optimal technology for their processing is a detailed analysis of their chemical and phase composition. And such analysis was the aim of the study the results of which are presented in this paper.

2. Materials and Methods

Forty slag samples were taken for testing from 4 layers from the entire profile of the Hazardous Waste Disposal Site of the Miasteczko Śląskie Zinc Smelting Plant. These layers differ in the age of the waste and the bottom layer is made up of the oldest slags and the top layer is made up of the youngest slags. These layers are separated by inert layers of granulated slag from the shaft process. The subject of research, the results of which are presented in this paper, were slags from the top layer (WI, WII, WIII, WIV), which represented the slag from current lead refining.

The chemical and phase composition of these samples was determined after averaging, grinding and preparation.

The chemical composition of the slag samples was determined by X-ray fluorescence (XRF) using a Panalytical Epsilon 1 spectrometer (Malvern Panalytical Ltd., Malvern, UK).

The X-ray phase analysis was performed on a Panalytical Empyrean diffractometer (Malvern Panalytical Ltd., Malvern, UK) under the following conditions—copper tube, voltage 30 kV, current 25 mA, 2θ scanning angle 5–100°.

Chemical composition was determined in a micro-area of the tested slag particles by means of a Jeol JCXA 733 X-ray microanalyzer (JEOL, Tokyo, Japan), equipped with an Oxford Instruments ISIS (Oxford Instruments, Abington, UK) 300 wave-length spectrometer (WDS) under the following conditions—focused beam (diameter: 1–2 μm, accelerating voltage 20 kV, current 3×10^{-9} A).The WDS method is characterized by high energy resolution, it means that the amount of overlap between peaks of similar energies is low.

The studies were mainly conducted on such grains that the beam did not extend beyond the grain outline, each wave spectrum measurement was preceded by the determination of the grain diameter. In the case of multiphase grains, the boundary between the intergrowth and the dominant phase was determined based on microscopic observations in reflected light. The series of ten microanalyses were carried out for each of the grains to determine the main chemical components and trace elements.

3. Results

3.1. Chemical Composition

3.1.1. Major Chemical Constituents

The major chemical constituents of the tested samples taken from the top layer of the landfill include FeO, PbO, CuO and SO_3 (Table 1). The total content of these constituents is over 74 wt %. The content of FeO is slightly diversified, ranging from 24.78 to 26.59 wt %., with an average of 25.75 wt %, which with the standard deviation of 0.75 gives a coefficient of variation (V) of 3%. The other main chemical constituents show a slightly greater diversity, viz.: PbO content varies from 14.96 to 21.72 wt % (V = 16%), CuO content varies from 13.57 to 20.68 wt % (V = 20%) and SO_3 content varies from 13.17 to 18.45 wt % (V = 14%).

Another significant constituent in terms of quantity is ZnO. Its content ranges from 9.59 to 11.53 wt %, which, with a relatively low value of the coefficient of variation (V = 9%), indicates its low differentiation.

Table 1. The chemical composition of the investigated samples WZI, WZII, WZIII and WZIV (in wt %).

Chemical Constituent	Sample Symbol				x	s	V
	WZI	WZII	WZIII	WZIV			
SiO_2	1.99 ± 0.20	2.98 ± 0.30	3.83 ± 0.39	4.99 ± 0.50	3.45	1.27	37
TiO_2	0.09 ± 0.02	0.14 ± 0.01	0.17 ± 0.02	0.15 ± 0.02	0.14	0.04	25
Al_2O_3	1.35 ± 0.14	2.97 ± 0.30	3.27 ± 0.33	3.56 ± 0.36	2.79	0.99	35
FeO	24.77 ± 1.24	25.94 ± 1.30	26.59 ± 1.33	25.70 ± 1.29	25.75	0.76	3
MnO	0.12 ± 0.01	0.57 ± 0.06	0.57 ± 0.06	0.56 ± 0.06	0.45	0.22	49
MgO	0.36 ± 0.04	0.59 ± 0.06	0.73 ± 0.08	0.50 ± 0.05	0.54	0.16	29
CaO	1.69 ± 0.17	4.75 ± 0.48	5.16 ± 0.52	4.42 ± 0.45	4.00	1.57	39
K_2O	0.05 ± 0.01	0.19 ± 0.02	0.23 ± 0.03	LLOD	0.12	0.11	94
P_2O_5	0.06 ± 0.01	0.08 ± 0.02	0.11 ± 0.01	0.09 ± 0.01	0.08	0.02	23
SO_3	17.54 ± 0.88	16.11 ± 0.08	18.45 ± 0.93	13.17 ± 0.66	16.32	2.31	14
ZnO	9.59 ± 0.96	11.53 ± 0.58	10.35 ± 0.52	11.50 ± 0.56	10.74	0.95	9
PbO	21.72 ± 1.09	18.76 ± 0.94	16.97 ± 0.85	14.96 ± 0.75	18.10	2.86	16
CuO	20.68 ± 1.03	15.39 ± 0.77	13.57 ± 0.68	20.40 ± 1.02	17.51	3.58	20
Total	100.00	100.00	100.00	100.00			
PbO + CuO + ZnO	51.99	45.68	40.89	46.87	46.36	4.56	10

x—average, s—standard deviation, V—coefficient of variation, LLOD—lower than limit of detection. The results are given with estimated uncertainties.

The content of the other chemical constituents is low. The average content of SiO_2, Al_2O_3 and CaO is a few wt %, whereas that of TiO_2, MnO, MgO, K_2O and P_2O_5 hardly exceeds 0.60 wt %.

Important information, arising from the chemical composition of the tested samples taken from the top layer of the landfill, is the total amount of metals that could be recovered. These constituents include PbO, CuO and ZnO, the total content of which ranges from 40.89 to 51.99 wt % and the value of the coefficient of variation V is 10%, which indicates a potential for their recovery.

3.1.2. Trace Elements

Among the trace elements, Ag, As, Ba, Bi, Cd, Co, Cr, In, Ni, Sb, Se and Tl were determined. The prevalence of As is evident, with its contents ranging from 0.94 to 1.33 wt %, hence in principle arsenic can be regarded as one of the major chemical constituents (Table 2).

Cadmium and antimony are the elements the contents of which are lower than that of arsenic but several times higher than that of the other. Their content ranges from 0.16 to 0.35 wt % for Cd and over 0.40 wt % for Sb. In the case of antimony, it should be pointed out that these are the values determined for two samples (WZI and WZII), as the content in the other samples was below the lower limit of detection.

The content of elements such as Ag, Ba, Co, Cr, In, Ni or Se does not exceed 0.05 wt % and in the case of Bi and Tl it is even less than 0.01 wt %. In addition, some of these elements are not present in all of the tested samples. This is especially true for bismuth and thallium, which were found only in sample WZI and for silver, which was found in samples WZI, WZII and WZVI.

Table 2. Trace elements content of the investigated samples WZI, WZII, WZIII and WZIV (in wt %).

Element	Sample Symbol			
	WZI	**WZII**	**WZIII**	**WZIV**
Ag	0.036 ± 0.006	0.009 ± 0.002	LLOD	0.018 ± 0.003
As	1.33 ± 0.14	1.24 ± 0.13	1.02 ± 0.11	0.94 ± 0.10
Ba	0.043 ± 0.007	0.035 ± 0.005	0.034 ± 0.005	0.053 ± 0.008
Bi	0.0086 ± 0.0017	LLOD	LLOD	LLOD
Cd	0.33 ± 0.04	0.35 ± 0.04	0.34 ± 0.04	0.16 ± 0.02
Co	0.045 ± 0.007	0.030 ± 0.005	0.030 ± 0.005	0.039 ± 0.006
Cr	0.039 ± 0.006	0.079 ± 0.012	0.064 ± 0.010	0.067 ± 0.011
In	0.048 ± 0.008	0.048 ± 0.008	0.031 ± 0.005	0.041 ± 0.007
Ni	0.043 ± 0.007	0.030 ± 0.005	0.030 ± 0.005	0.031 ± 0.005
Sb	0.44 ± 0.05	0.43 ± 0.05	LLOD	LLOD
Se	0.034 ± 0.006	0.028 ± 0.005	0.027 ± 0.004	0.028 ± 0.005
Tl	0.0086 ± 0.0019	LLOD	LLOD	LLOD

LLOD—lower than limit of detection. The results are given with estimated uncertainties.

3.2. Phase Composition

3.2.1. Major Phase Constituents

The main phase constituents present in the charge mixture as shown in the studies [17,18] included galena PbS, sphalerite ZnS, iron sulphides, zincite ZnO, anglesite $PbSO_4$, lead oxide PbO, FeO–ZnO oxides and glass. They were included in the feedstock for the process (zinc blend concentrate, galena concentrate) and other constituents, which formed the charge mixture, such as—semi-finished products (Zn–Pb sinters), waste (dust, dross, slag), products from the process (crude zinc, crude lead). Yet in the composition of the main phases of the tested samples taken from the top layer of the landfill, as indicated by the present studies, only anglesite (lead sulphate), sphalerite (zinc sulphide) and glass were present among the phases of the charge mixture. However, new phases formed during the process and resulting from hypergenic transformations of these phases, taking place in the landfill, were also found. Among the phases found in the tested samples of the top layer of the landfill, the following groups were distinguished:

- silicates—kirschsteinite $CaFeSiO_4$, willemite Zn_2SiO_4,
- sulphates and hydrated sulphates—anglesite $PbSO_4$, gypsum $CaSO_4{\cdot}2H_2O$, ktenasite$ZnCu_4(SO_4)_2(OH)_6{\cdot}6H_2O$, namuvite $Zn_4(SO_4)(OH)_6{\cdot}4H_2O$, tochilinite $Fe^{2+}{}_{5–6}(Mg,Fe^{2+})_5S_6(OH)_{10}$,
- nitrates—gerhardtite $Cu_2(NO_3)(OH)_3$,
- sulphides and metals—sphalerite ZnS, metallic Pb,
- oxides and hydroxides—goethite FeO(OH), wustite FeO,
- glass.

The presence of these phases is evidenced by the characteristic reflections in the diffractograms of the tested samples (Figure 1). Worth noting is the varied intensity of some basic reflections in the diffractograms, assigned to individual phases, which indicates different content of these in the tested samples.

The study of the chemical composition in the micro-areas revealed that the grains of the main phases formed intergrowths of very small clusters of individual phases. Grains composed of one phase only occur very rarely. The determined chemical composition of the grains of the main phase in the tested samples indicates that in some cases admixtures of various elements, mainly metals, are present. It was found, for instance, that:

- wustite (Figure 2, Table 3) may contain admixtures of Zn (up to 5.68 wt %), Cu (up to 5.59 wt %), Sn (up to 1.61 wt %), Sb (up to 2.09 wt %) and of Pb (2.95 wt %),

– kirschsteinite (Figure 3, Table 3) contained Zn (up to 6.17 wt %), Pb (up to 2 wt %), Cu (up to 1.12 wt %), Mn (up to 0.83 wt %).

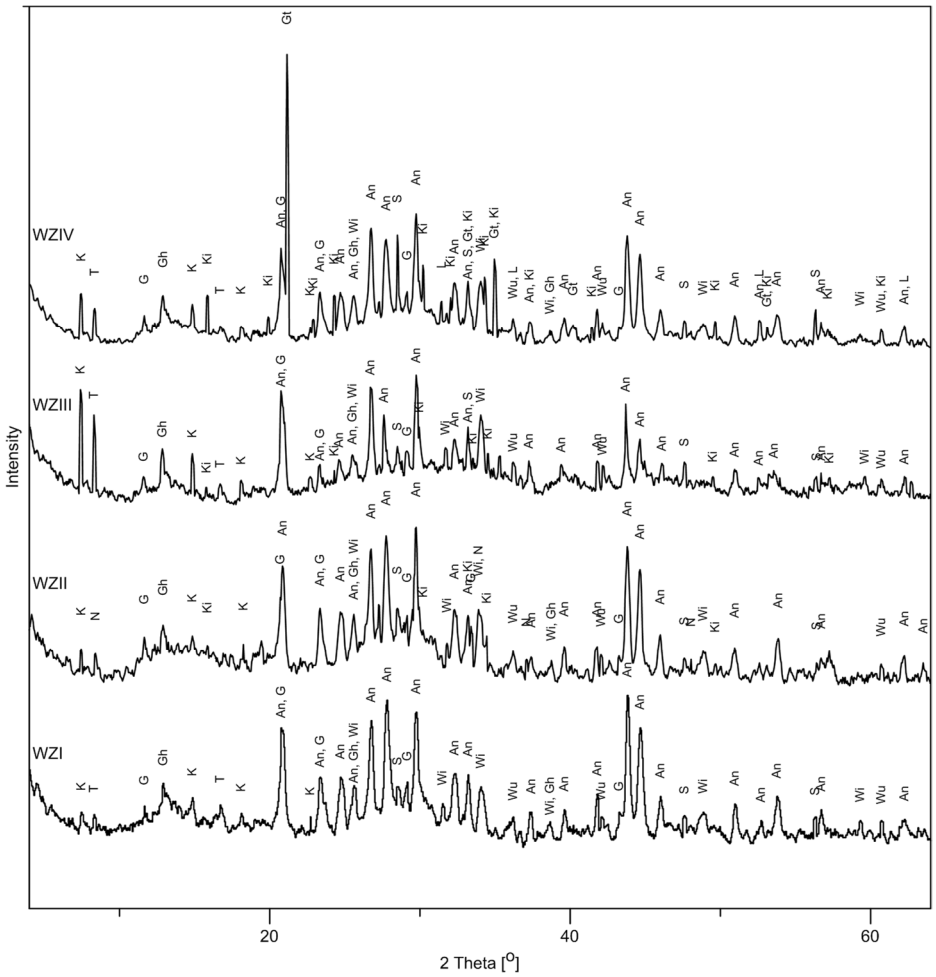

Figure 1. X-ray diffraction (XRD) patterns of samples WZI, WZII, WZIII and WZIV. Explanation: An-anglesite, G—gypsum, Gh—gerhardtite, Gt—goethite, Ki—kirschsteinite, K—ktenasite, L—metallic Pb, N—namuvite, S—sphalerite, T—tochilinite, Wi—willemite, Wu—wustite.

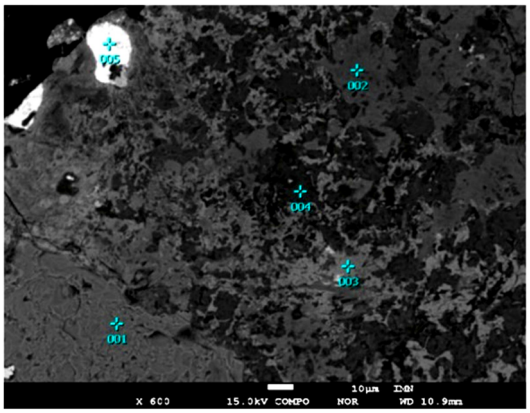

Figure 2. Sample WZI—example of an image of the investigated micro-areas. 1—wustite with Zn admixture (9%), 2—wustite with silicate admixtures, 3 and 4—wustite with Sb admixture (17–22%), 5—Pb oxide.

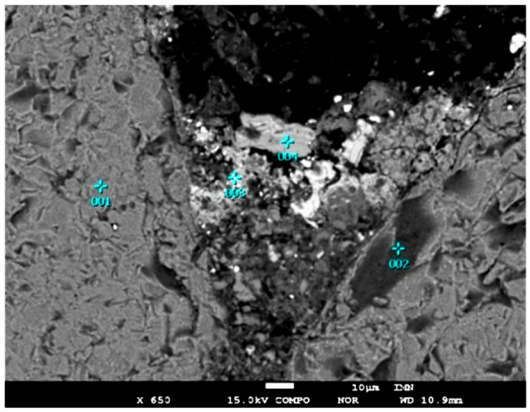

Figure 3. Sample WZIII - example of an image of the investigated micro-areas. 1—kirschsteinite with wustite, 2—glass, 3—Pb-Cu alloy with Au admixture (6%), 4—Pb–Fe–Zn.

Table 3. Differentiation of the chemical composition of wustite and kirschsteinite, occurring in the investigated grains of samples taken from the top layer of the landfill.

Element	Wustite					Kirschsteinite				
	Min	**Max**	***x***	***s***	***V***	**Min**	**Max**	***x***	***s***	***V***
O	21.20	22.98	22.10	0.55	2	28.67	33.67	31.92	1.85	6
Na						0.00	0.60	0.15	0.25	168
Mg	0.00	1.96	0.50	0.63	124	1.01	2.04	1.25	0.39	31
Al	0.00	0.51	0.22	0.18	83	1.20	3.70	2.44	0.90	37
Si						12.79	14.72	13.74	0.81	6
K						0.00	0.70	0.35	0.22	64
Ca	0.00	0.89	0.23	0.32	141	14.30	18.79	16.39	1.97	12
Mn	0.00	0.17	0.02	0.05	268	0.00	0.83	0.51	0.31	60
Fe	61.00	77.39	71.01	4.81	7	25.43	29.87	27.90	1.63	6
Cu	0.00	5.59	1.87	1.93	104	0.00	1.12	0.45	0.47	103
Zn	0.00	5.68	1.84	1.97	107	0.19	6.17	2.90	2.36	81
Ag	0.00	0.20	0.05	0.07	146	0.00	0.07	0.01	0.03	245
Cd	0.00	0.21	0.05	0.09	186	0.00	0.30	0.07	0.12	163
As	0.00	0.06	0.01	0.02	212	0.00	0.58	0.22	0.26	117
In	0.00	0.40	0.06	0.13	217	0.00	0.81	0.46	0.34	73
Sn	0.00	1.61	0.35	0.48	138					
Sb	0.00	2.09	0.37	0.66	180	0.00	0.70	0.27	0.24	91
Pb	0.00	2.95	1.33	0.98	73	0.12	2.00	0.95	0.61	64

Min—minimum, Max—maximum, x—average, s—standard deviation, *V*—coefficient of variation.

There are two characteristic relationships in the chemical composition of wustite. With increasing iron content, the content of copper and zinc decrease (Figures 4 and 5). At the same time the R^2 value of the trend line is very high: 0.74 for Cu and 0.83 for Zn. Therefore, it can be concluded that both copper and zinc substitute iron in wustite, which is quite common in this type of iron oxides [19–22].

There are a few characteristic relationships in the chemical composition of kirschsteinite:

– with increasing silicon content, the content of aluminum decreases and the R^2 value of the trend line is in this case 0.97 (Figure 6),
– with increasing iron content:

  - the content of copper and calcium increases and the R^2 value of the trend line is 0.87 for Cu (Figure 7) and 0.85 for Ca (Figure 8), respectively,
  - the content of zinc decreases and the R^2 value of the trend line is 0.94 (Figure 9),

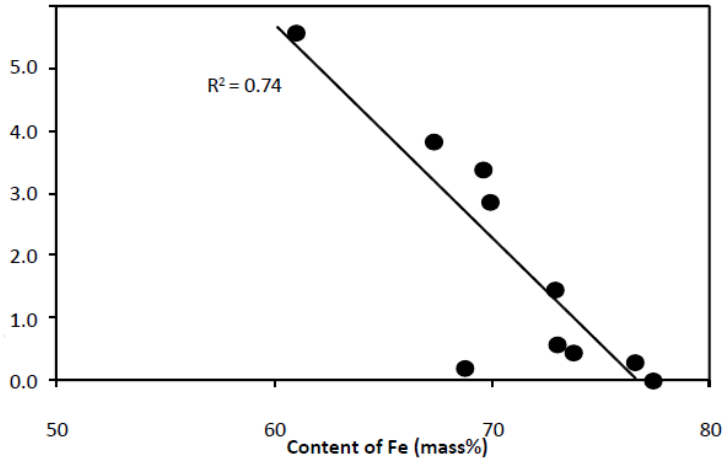

Figure 4. Differentiation of Fe and Cu content in wustite.

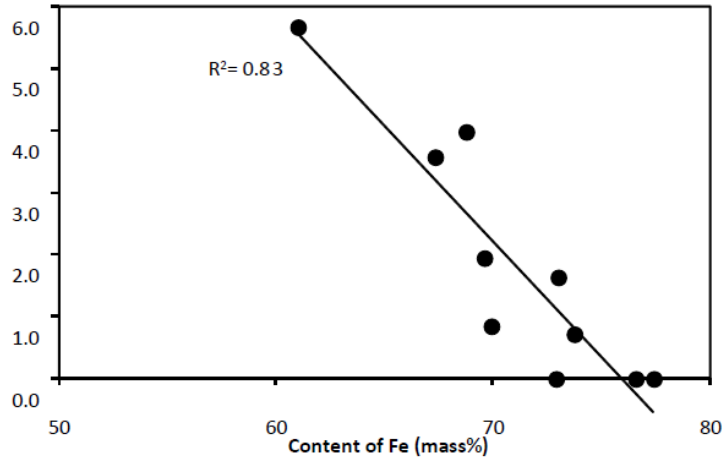

Figure 5. Differentiation of Fe and Zn content in wustite.

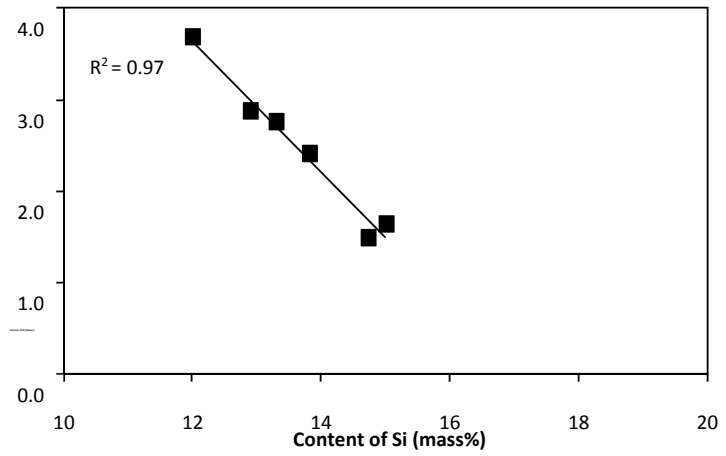

Figure 6. Differentiation of Si and Al content in kirschsteinite.

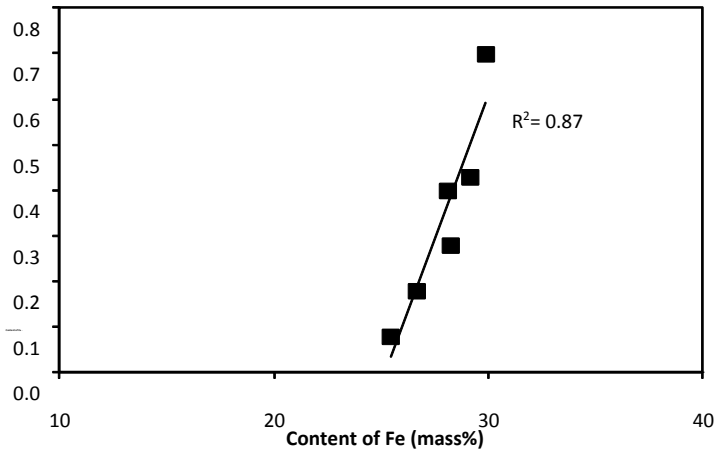

Figure 7. Differentiation of Fe and Cu content in kirschsteinite.

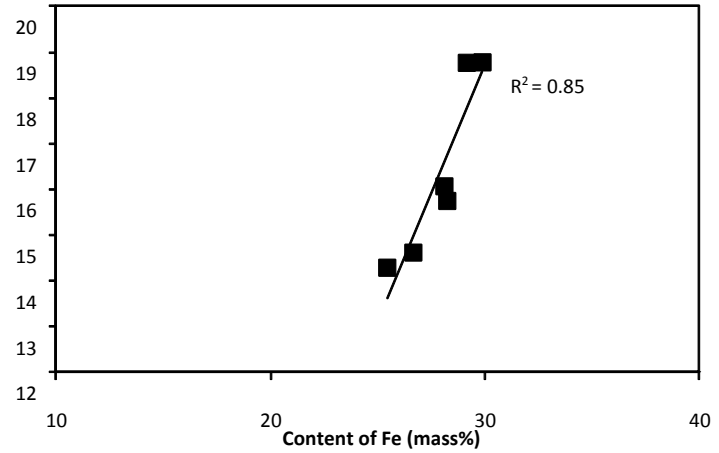

Figure 8. Differentiation of Fe and Ca content in kirschsteinite.

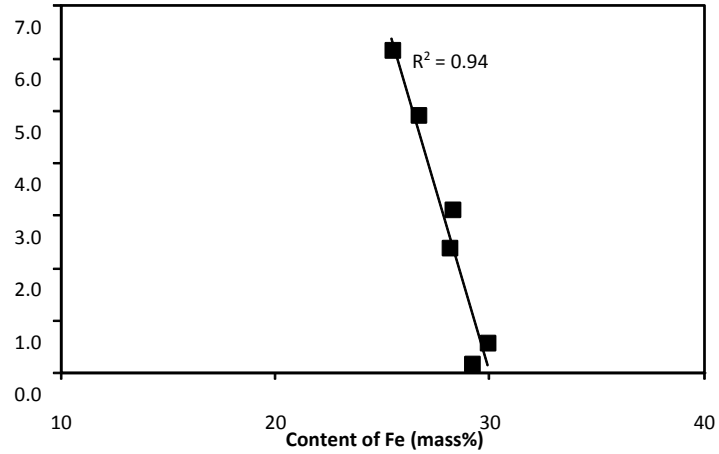

Figure 9. Differentiation of Si and Zn content in kirschsteinite.

The relationship between silicon and aluminum may indicate a diadochal substitution of silicon and aluminum, due to their crystallographic similarity (similar ionic radius), which is quite common in silicates [23]. In turn, the relation between Ca and Fe is also geochemically justified in the group of minerals to which kirschsteinite belongs [24–27].

However, the relations between copper and zinc and iron in kirschsteinite are interesting in the context of those previously determined in wustite. Although the zinc content in both phases decreases

with increasing iron content, the copper content in kirschsteinite increases while in wustite it decreases. It is difficult to explain this phenomenon conclusively.

Thus, among the phase constituents of the examined waste of the top layer, three types can be distinguished, taking into account their origin:

- mineral constituents, which are part of zinc and lead concentrates used as feedstock in the pyrometallurgical process—this includes sphalerite only,
- phase constituents formed in the technological process—these include mainly kirschsteinite and wustite,
- secondary mineral constituents, formed in the landfill under the action of hypergenic factors—these include gypsum, ktenasite, namuvite, tochilinite, gerhardtite, goethite.

Anglesite, willemite, metallic lead and glass may be of problematic origin, as on the one hand they may belong to the type of mineral constituents contained in small quantities in zinc and lead concentrates (anglesite and willemite) and on the other hand to the type of phase constituents formed in the technological process which are returned to the process (anglesite, metallic lead, glass).

As indicated by numerous studies, gypsum, ktenasite, namuvite, tochilinite, gerhardtite, goethite are known to be present as secondary phases in many deposits and landfills of metallurgical plants, among others—the Remšnik ore deposit (Slovenia), the Upper Silesian Mississippi Valley-type deposits (MVT) (Poland), the Aznalcóllar deposit (Spain), the Świętochłowice Dump (Poland), the base-metal slag deposits at the Penn Mine in Calaveras County (USA) [24–32].

3.2.2. Trace Phases

The results of chemical composition analysis of the grains in micro-areas revealed the presence of phases which are present in much smaller quantities and which therefore did not exhibit their characteristic reflections in the X-ray diffractograms. As in the case of the main phases, the phases occurring in trace quantities do not form individual grains. Usually they form small size inclusions in the main phases or occur at the border of the main phases.

These phase constituents include—Pb oxides, which sometimes form intergrowths with wustite FeO (Figures 10 and 11), quartz SiO_2, cerussite $PbCO_3$, alamosite$Pb_{12}Si_{12}O_{36}$ (Figure 12), bornite Cu_5FeS_4, metallic Ag and metal alloys (Cd-Zn, Pb-Cu, Zn-Cu, Pb-Fe-Zn, Pb-Fe-Cu, Pb-Fe-Sb, Sn-Zn-Pb) (Table 4). Some grains are equivalent, in terms of chemical composition, to franklinite $ZnFe_2O_4$, sometimes with admixtures of leiteite $ZnAs_2O_4$ and to Pb oxide with admixtures of paulmooreite$Pb_2(As_2O_5)$ (Figure 13).

As in the case of the main phase constituents, among the phase constituents present in trace amounts in the examined waste of the top layer, three types can be distinguished, taking into account their origin:

- mineral constituents, which are part of zinc and lead concentrates used as feedstock in the pyrometallurgical process—these probably include alamosite, quartz and cerussite, which are contaminants of the concentrates resulting from the mineralization of the Zn-Pb ore deposits from which the concentrates are derived,
- phase constituents formed in the technological process—these probably include metal alloys, Pb oxides and metallic Ag,
- secondary mineral constituents, formed in the landfill under the action of hypergenic factors—these probably include leiteite and paulmooreite.

Table 4. Examples of chemical compositions of some phase constituents present in the investigated grains of samples taken from the top layer of the landfill.

Element	Cerussite	Pb Oxide		Cu and Fe Sulphides			AnCe	Alloys				
								Pb–Fe(Sb)	Zn–Cu	Pb–Fe–Cu		Ag
C	4.3						14.9					
O	12.3	4.7	6.3				7.5	14.0	4.1	12.2	11.7	
Na	2.0							1.2				
Mg				0.1						0.2		
Al			0.5	1.0				0.6		0.4	0.7	0.8
Si			3.8	1.3				2.2		2.2		0.7
S				21.8	30.0	26.1	9.3		1.9	1.0	2.6	
K												
Ca												1.3
Mn												
Fe		1.1		16.1	21.9	10.5		14.8	2.8	16.2	11.8	2.9
Cu				54.1	40.7	58.5			41.6	11.9	8.9	0.0
Zn				1.1	3.2				49.6	8.7	2.9	0.0
Ag				0.4	0.2							94.3
Cd					0.3		1.1			0.4		
As			4.0	0.1	0.0							
In					1.7					0.4		
Sn	1.7	1.8	2.0	0.3		0.3	1.2			1.2	1.1	
Sb	2.9	3.8	1.3	0.3	0.3	0.3	2.8	23.1		2.8	2.5	
Pb	76.8	88.6	82.1	3.4	1.7	4.3	63.2	44.2		42.5	57.8	
	100.0	100.0	100.0	100.0	100.0	100.0	100.0	100.0	100.0	100.0	100.0	100.0

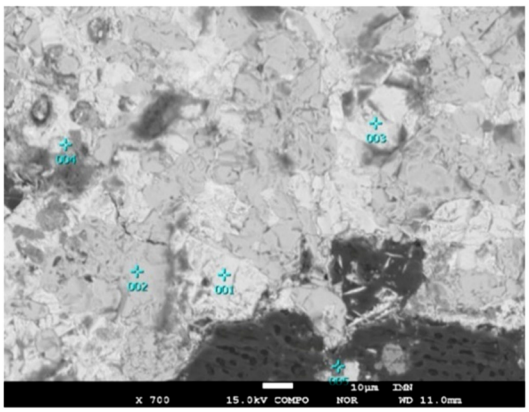

Figure 10. Sample WZI—example of an image of the investigated micro-areas. 1 and 3—Pb oxide, 2—Pb oxide with willemite, 4—gerhardtite, 5—wustite.

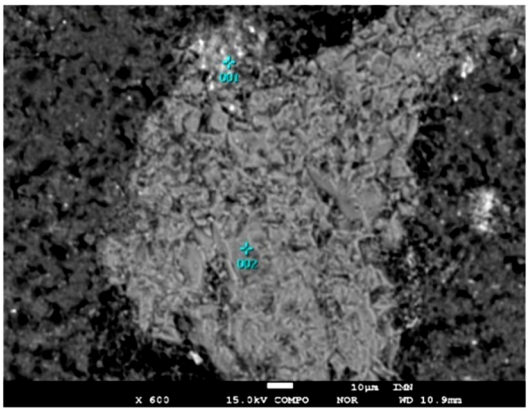

Figure 11. Sample WZII—example of an image of the investigated micro-areas. 1—wustite with Pb oxide, 2—kirschsteinite.

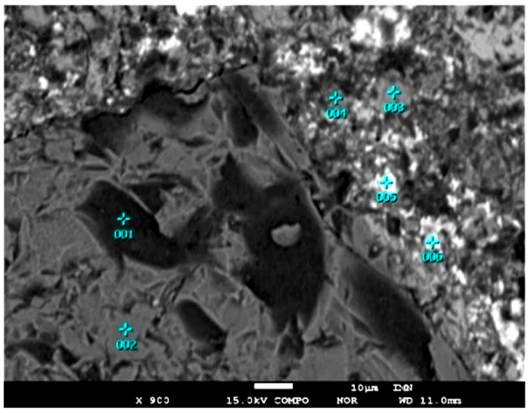

Figure 12. Sample WZIII—example of an image of the investigated micro-areas. 1—quartz, 2—kirschsteinite with wustite, 3—Sn-Zn-Pb alloy, 4—glass with alamosite, 5 and 6—alamosite in glass.

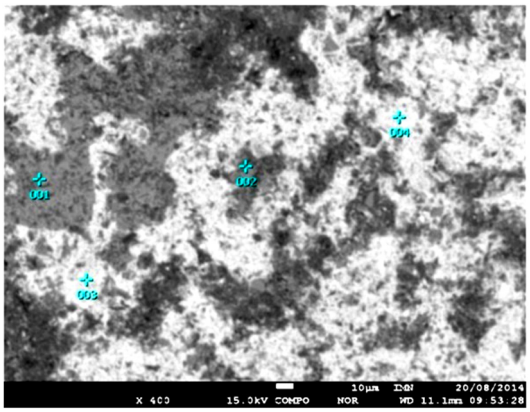

Figure 13. Sample WZIV—example of an image of the investigated micro-areas. 1—leiteite with franklinite, 2—franklinite, 3 and 4—Pb oxide with paulmooreite.

The provenance of franklinite and bornite may be problematic. They may belong to the group of mineral constituents contained in small quantities in zinc and lead concentrates or to the group of phase constituents formed in the technological process which are returned to the process.

As indicated by numerous studies, both leiteite and paulmooreite are known to be present as secondary phases in many deposits and landfills of metallurgical plants (the Tsumebdeposite, Namibia; Bushveld Complex, South Africa) [33–35].

4. Discussion

The identification of the main phases by X-ray diffraction and the established chemical composition of the tested samples allowed to calculate the content of these phases and the results of these calculations are presented in Table 5.

The dominant phases in the samples are anglesite, gerhardtite and wustite, the total content of which varies from about 52% to about 68 wt %, with the exception of the WZIV sample, where the total of these three constituents is 27.50 wt %. In that sample, kirschsteinite, ktenasite and goethite are significant in quantitative terms.

It can therefore be concluded that the samples are quite diverse in terms of phases and in particular in terms of the proportion of individual phases. And although it seems that samples WZI, WZII and WZIII are very similar to each other as compared to WZIV, they still show quite strong qualitative differences between them. This is manifested, for instance, in the presence of:

– namuvite in sample WZII, whereas samples WZI, WZIII and WZIV do not contain this phase,
– tochilinite in samples WZI, WZIII and WZIV, whereas sample WZII does not contain this phase,

– metallic Pb and goethite in sample WZIV, whereas these constituents are not present in any of the other samples,
– kirschsteinite in all samples, except WZI.

Table 5. The main phases content of the investigated samples WZI, WZII, WZIII and WZIV (in wt %).

Phase Type	Phase	Sample Symbol				*x*	*s*	*V*
		WZI	WZII	WZIII	WZIV			
Primary	Sphalerite	8.39	5.23	5.91	7.08	6.65	1.39	21
	Anglesite	25.63	22.83	22.40	10.41	20.32	6.76	33
	Willemite	8.53	4.51	6.24	3.94	5.81	2.06	36
Process	Kirschsteinite		3.46	4.88	14.73	5.77	6.32	110
	Wustite	22.61	22.24	20.08	1.99	16.73	9.89	59
	Metallic Pb				6.97			
	Glass	5.08	5.19	6.24	6.03	5.64	0.59	10
Secondary	Gypsum	3.98	8.64	9.76	3.24	6.41	3.27	51
	Ktenasite	2.78	2.55	8.22	13.77	6.83	5.32	78
	Namuvite		16.54					
	Tochilinite	2.95		6.00	4.14	3.27	2.52	77
	Gerhardtite	20.05	8.81	10.27	15.10	13.56	5.10	38
	Goethite				12.60			
Total		100.00	100.00	100.00	100.00			
Phase group								
Silicates		8.53	7.97	11.12	18.67	11.57	4.93	43
Sulphates		32.39	50.56	40.38	27.42	37.69	10.11	27
Nitrates		20.05	8.81	10.27	15.10	13.56	5.10	38
Sulphides and hydrated sulphides		11.34	5.23	11.91	11.22	9.93	3.14	32
Oxides and hydroxides		22.61	22.24	20.08	14.59	19.88	3.70	19
Metals		0.00	0.00	0.00	6.97	1.74	3.49	200
Glass		5.08	5.19	6.24	6.03	5.64	0.59	10
Total		100.00	100.00	100.00	100.00			

x—average, *s*—standard deviation, *V*—coefficient of variation.

The quantitative variation of the phases occurring in all samples is manifested, among others, in the content of—kirschsteinite (0–14.73 wt %, V = 110%), ktenasite (2.55–13.77 wt %, V = 78%), tochilinite (0–6.00 wt %, V = 77%) and wustite (1.99–22.61 wt %, V = 59%). The constituents that exhibit the least content variation are glass (5.08–6.24 wt %, V = 10%) and sphalerite (5.23–8.39 wt %, V = 21%).

The three distinguished types of phases (primary constituents, which form the feedstock in the process; constituents formed in the course of the process; secondary constituents, formed in the landfill under the action of hypergenic factors) are set out in a diagram (Figure 14). In the tested waste of the top layer, three samples (WZI, WZII and WZIII) are located in the middle of the diagram, which suggests similar content of these three types of phases, while the location of the projection point of the WZIV sample indicates a dominant content of secondary constituents. It will be noted, however, that in the waste under investigation there are still significant amounts of primary constituents, that is, feedstock in the process, which can be reused for metal recovery, like the other constituents. An important element of this recovery is certainly the content of metals in these constituents.

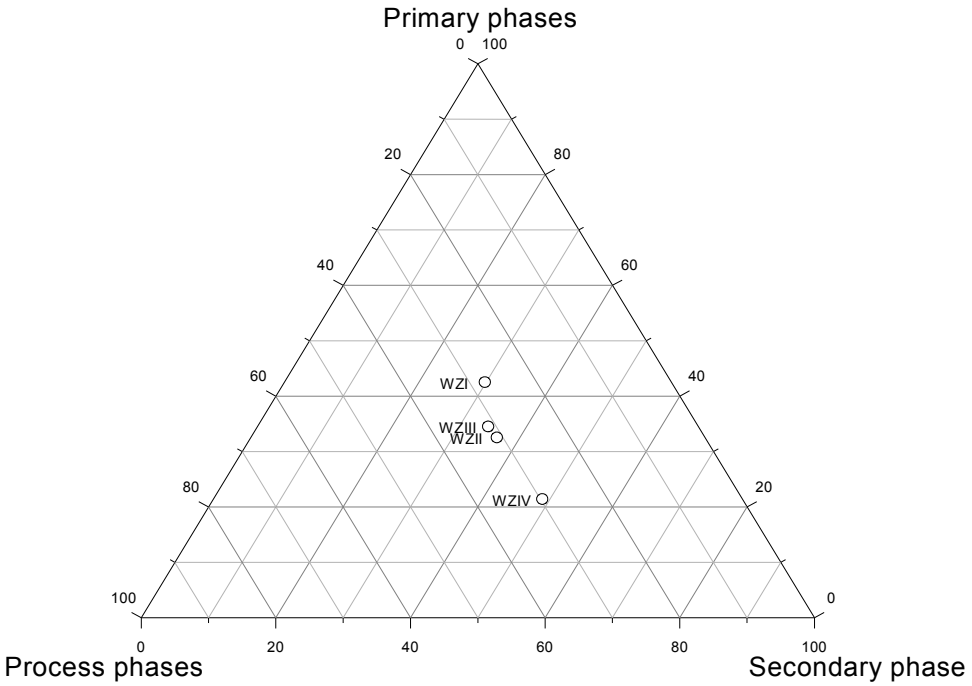

Figure 14. Diagram of phases of the investigated samples WZI, WZII, WZIII and WZIV.

However, from the point of view of the recoverability of metals, it is more important to consider the quantitative aspects of individual phases, grouped in the form of chemical compounds or the classification of minerals used in mineralogy, which illustrates the forms of metal occurrence. For this reason, the phases occurring in the tested samples were divided into 7 groups—(i) silicates, (ii) sulphates and hydrated sulphates, (iii) nitrates, (iv) sulphides and hydrated sulphides, (v) oxides and hydroxides, (vi) metals and (vii) glass (Table 5).

Sulphates and hydrated sulphates (anglesite, gypsum, ktenasite and namuvite) show the highest content in the tested samples, at an average content of about 38 wt %. The second group in terms of quantity are oxides and hydroxides (wustite and goethite), with their average content close to 20 wt %. The content of nitrates (gerhardtite) and silicates (kirschsteinite and willemite) are comparable, the average figures being 13.56 and 11.57 wt %, respectively. Average content of the other phase groups is below 10 wt % and these include sulphides and hydrated sulphides (sphalerite and tochilinite, average content 9.93%), metals (metallic Pb, average content 1.74 wt %) and glass (average content 5.64%).

A very important factor that must be considered in the technological recovery of metals (Pb, Cu and Zn) is their content in the individual phases.

5. Conclusions

Refining slags deposited in the top layer of the Hazardous Waste Disposal Site are characterized by varied development of the phase constituents and hence—(i) the main phases are usually in the form of conglomerates or multiphase intergrowths, (ii) trace elements form small size inclusions in the main phases or occur at their border.

The predominant phase constituents in the tested slags include—sulphates and hydrated sulphates (anglesite, gypsum, ktenasite and namuvite) at an average content of ca. 38 wt %, oxides and hydroxides (wustite and goethite) at an average content close to ca. 20 wt %, nitrates (gerhardtite) and silicates (kirschsteinite and willemite) at an average content of 13.56 and 11.57 wt %, respectively. Average content of the other phase groups is below 10 wt % and these include sulphides and hydrated sulphides (sphalerite and tochilinite), metals (metallic Pb) and glass.

Among the main and trace phase constituents of refining slags, the following can be identified—(i) primary mineral constituents, which are part of Zn-Pb concentrates (sphalerite, alamosite, quartz

and cerussite), (ii) phase constituents formed in the ISP process and during chemical transformations occurring in the course of lead refining (kirschsteinite, wustite, metal alloys, Pb oxides and metallic Ag), (iii) secondary mineral constituents, formed in the landfill under the action of hypergenic factors (gypsum, ktenasite, namuvite, tochilinite, gerhardtite, goethite, leiteite and paulmooreite).

The major chemical constituents of the tested samples taken from the top layer of the landfill include FeO, CuO and SO_3, PbO, the total content of which is over 74 wt %. Constituents found at substantially lower concentrations include SiO_2, Al_2O_3 and CaO, TiO_2, MnO, MgO, K_2O, P_2O_5. The content of the main constituents shows little variation, as the coefficient of variation V is below 22%.

Both the high content of metals, Zn, Pb, with their low variability and the significant content thereof in the individual phases, as well as their presence in the primary constituents, make refining slags a potential source of these metals and pyrometallurgical processing of these wastes seems to be highly rational.

Funding: An article processing charge was funded by Rector's Grant of the Silesian University of Technology, grant number 06/060/RGH19/0079.

Acknowledgments: I gratefully thank Z. Adamczyk for the discussion and valuable suggestions while writing this article.

Conflicts of Interest: The author declare no conflict of interest.

References

1. Vignes, A. *Extractive Metallurgy 3*; Willey: Hoboken, NJ, USA, 2013.
2. Potesser, M.; Holleis, B.; Antrekowitsch, H.; Konetschnik, S. New Pyrometallurgical Bullion Lead Refining Process. In Proceedings of the TMS 2008, 137th Annual Meeting & Exhibition, New Orleans, LA, USA, 9–13 March 2008; pp. 1–8.
3. Chodkowski, S. *Metalurgia Metali Nieżelaznych*; Wydawnictwo Śląsk: Katowice, Poland, 1971.
4. Adamczyk, Z.; Nowińska, K. Phase composition of metallurgical zinc and lead slags. *Civil Environ. Eng. Rep.* **2013**, *11*, 13–21.
5. Nowińska, K.; Adamczyk, Z. Slags of the imperial smelting process for Zn and Pb production. In *Reference Module in Materials Science and Materials Engineering*; Saleem, H., Ed.; Elsevier: Amsterdam, The Netherlands, 2017; pp. 1–5.
6. Lima, L.R.P.D.A.; Bernardez, L. Characterization of the lead smelter slag in Santo Amaro, Bahia, Brazil. *J. Hazard. Mater.* **2011**, *189*, 692–699. [CrossRef] [PubMed]
7. Ettler, V.; Johan, Z.; Touray, J.-C.; Jelínek, E. Zinc partitioning between glass and silicate phases in historical and modern lead–zinc metallurgical slags from the Příbram district, Czech Republic. *Earth Planet. Sci.* **2000**, *331*, 245–250. [CrossRef]
8. Ettler, V.; Komárková, M.; Jehlicka, J.; Coufal, P.; Hradil, D.; Machovič, V.; Delorme, F. Leaching of lead metallurgical slag in citric solutions—implications for disposal and weathering in soil environments. *Chemosphere* **2004**, *57*, 567–577. [CrossRef]
9. Harvey, W.; Downs-Rose, G. The Bay Mine, Wanlockhead, Scotland. *Br. Min.* **1976**, *2*, 1–9.
10. Kierczak, J.; Puziewicz, J.; Bril, H. Pyrometallurgical Slags in Upper and Lower Silesia (Poland): From Environmental Risks to Use of Slag-based Products—A Review. *Arch. Environ. Prot.* **2010**, *36*, 111–126.
11. Kucha, H.; Martens, A.; Ottenburgs, R.; De Vos, W.; Viaene, W. Primary minerals of Zn-Pb mining and metallurgical dumps and their environment behavior at Plombieres, Belgium. *Environ. Geol.* **1996**, *27*, 1–7. [CrossRef]
12. Paar, W.H.; Mereiter, K.; Braithwaite, R.S.W.; Keller, P.; Dunn, P.J. Chenite, $Pb_4Cu(SO4)_2(OH)_6$, a new mineral, from Leadhills, Scotland. *Miner. Mag.* **1986**, *50*, 129–135. [CrossRef]
13. Piatak, N.M.; Seal, R., II. Mineralogy and the release of trace elements from slag from the Hegeler Zinc smelter, Illinois (USA). *Appl. Geochem.* **2010**, *25*, 302–320. [CrossRef]
14. Warchulski, R.; Doniecki, T.; Gawęda, A.; Szopa, K. Composition and weathering of Zn-Pb slags from Bytom—PiekaryŚląskie area: A case of heavy metal concentration and mobility. *Mineral. Spec. Pap.* **2012**, *40*, 132–133.

15. Warchulski, R.; Doniecki, T.; Gawęda, A.; Szopa, K. Secondary phases from the Zn-Pb smelting slags from Katowice—Piekary Śląskie area, Upper Silesia, Poland: A SEM—XRD overview. *Mineral. Spec. Pap.* **2014**, *42*, 110.
16. Warchulski, R.; Gawęda, A.; Kądziołka-Gaweł, M.; Szopa, K. Composition and element mobilization in pyrometallurgical slags from the Orzeł Biały smelting plant in the Bytom–Piekary Śląskie area, Poland. *Miner. Mag.* **2015**, *79*, 459–483. [CrossRef]
17. Pozzi, M.; Nowińska, K. *Dystrybucja Wybranych Pierwiastków Towarzyszących Koncentratom Zn-Pb w Technologii Imperial Smelting Process*; Wydawnictwo Politechniki Śląskiej: Gliwice, Poland, 2006.
18. Adamczyk, Z.; Melaniuk-Wolny, E.; Nowińska, K. *The Mineralogical and Chemical Study of Feedstock Mixtures and by-Products from Pyrometallurgical Process of Zinc and Lead Production*; Wydawnictwo Politechniki Śląskiej: Gliwice, Poland, 2010.
19. Billon, G.; Ouddane, B.; Recourt, P.; Boughriet, A. Depth Variability and some Geochemical Characteristics of Fe, Mn, Ca, Mg, Sr, S, P, Cd and Zn in Anoxic Sediments from Authie Bay (Northern France). *Estuar. Coast. Shelf Sci.* **2002**, *55*, 167–181. [CrossRef]
20. Karbassi, A.R. Geochemistry of Ni, Zn, Cu, Pb, Co, Cd, V, Mn, Fe, Al and Ca in sediments of North Western part of the Persian Gulf. *Int. J. Environ. Stud.* **1998**, *54*, 205–212. [CrossRef]
21. Rose, A.W. Geochemical methods of prospecting for non-metallic minerals. *J. Geochem. Explor.* **1991**, *41*, 387–388. [CrossRef]
22. Cappuyns, V.; Alian, V.; Vassilieva, E.; Swennen, R. pH Dependent Leaching Behavior of Zn, Cd, Pb, Cu and As from Mining Wastes and Slags: Kinetics and Mineralogical Control. *Waste Biomass. Valorization* **2013**, *5*, 355–368. [CrossRef]
23. Handke, M. *Krystalochemia Krzemianów*; Uczelniane Wydawnictwo Naukowo-Dydaktyczne AGH: Kraków, Poland, 2005.
24. Cairncross, B.; Windisch, W. Microminerals from Bushveld Complex South Africa. *Mineral. Rec.* **1998**, *29*, 461–466.
25. Trajanova, M.; Žorž, Z. Abandoned Remšnik mine with ramsbeckite and namuwite(?). *Geologija* **2013**, *56*, 57–72. [CrossRef]
26. Groat, L.A. The crystal structure of namuwite, a mineral with Zn in tetrahedral and octahedral coordination, and its relationship to the synthetic basic zinc sulfates. *Am. Miner.* **1996**, *81*, 238–243. [CrossRef]
27. Bevins, R.E.; Turgoose, S.; Williams, P.A. Namuwite, (Zn,Cu)4SO4(OH)6.4H2O, a new mineral from Wales. *Miner. Mag.* **1982**, *46*, 51–54. [CrossRef]
28. Martín, F.; Diez, M.; García, I.; Simón, M.; Dorronsoro, C.; Iriarte, Á.; Aguilar, J.; Martín-Peinado, F. Weathering of primary minerals and mobility of major elements in soils affected by an accidental spill of pyrite tailing. *Sci. Total. Environ.* **2007**, *378*, 49–52. [CrossRef] [PubMed]
29. Bril, H.; Zainoun, K.; Puziewicz, J.; Courtin-Nomade, A.; Vanaecker, M.; Bollinger, J.-C. Secondary phases from the alteration of a pile of zinc-smelting slag as indicators of environmental conditions: An example from swietochlowice, upper silesia, poland. *Can. Miner.* **2008**, *46*, 1235–1248. [CrossRef]
30. Parsons, M.; Bird, D.K.; Einaudi, M.T.; Alpers, C.N. Geochemical and mineralogical controls on trace element release from the Penn Mine base-metal slag dump, California. *Appl. Geochem.* **2001**, *16*, 1567–1593. [CrossRef]
31. Bauerek, J.; Cabala, B. Smieja-Król, Mineralogical Alterations of Zn-Pb Flotation Wastes of the Mississippi Valley Type Ores (Southern Poland) and Their Impact on Contamination of Rain Water Runoff. *Polish J. Environ. Stud.* **2009**, *18*, 781–788.
32. Cabała, J. *Metale Ciężkie w Środowisku Glebowym Olkuskiego Rejonu Eksploatacji Rud Zn-Pb*; Wydawnictwo Uniwersytetu Śląskiego: Katowice, Poland, 2009.
33. Bowell, R.J.; Mocke, H. Minerals new to Tsumeb. *Commun. Geol. Surv. Namib.* **2018**, *19*, 20–46.
34. Majzlan, J.; Drahota, P.; Filippi, M. Parageneses and Crystal Chemistry of Arsenic Minerals. *Rev. Miner. Geochem.* **2014**, *79*, 17–184. [CrossRef]
35. Bohlke, J.; Friedrich, B.; Hecker, E. Treatment of Industrial Lead and Zinc Slags in a Pilot Scale SAF. World Metall. *Erzmetall* **2005**, *58*, 210–217.